

The pH Dependence of the Ca^{2+} , Mg^{2+} -ATPase of Sarcoplasmic Reticulum: Evidence that the Ca^{2+} Translocator Bears a Doubly Negative Charge

Duncan H. Haynes and Alan Mandveno

Department of Pharmacology, University of Miami Medical School, Miami, Florida 33101

Summary. The pH dependence of the Ca^{2+} , Mg^{2+} -ATPase pump of rabbit skeletal sarcoplasmic reticulum has been analyzed. Active uptake progress curves of the free luminal Ca^{2+} concentration *vs.* time were obtained by fluorometric readout. The average rates (evaluated at $t = 2$ sec) and steady-state maximal uptakes ($[\text{Ca}^{2+}]_i$) were determined at variable external $[\text{Ca}^{2+}]_o$, set by a Ca^{2+} /EGTA buffer. The average rates ($t = 2$ sec) and the $[\text{Ca}^{2+}]_i$ values showed the same dependence on $[\text{Ca}^{2+}]_o$ and pH. At pH 7.0, a second-order dependence on $[\text{Ca}^{2+}]_o$ was observed with a K_m (equal to $[\text{Ca}^{2+}]_i$ for half-maximal rate) of 7.3×10^{-8} M. Both the average rate and the maximal internal Ca^{2+} level achieved had identical K_m values. The apparent affinity of the pump for Ca^{2+} ($K_{\text{app}} = 1/K_m$) shows little pH dependence between pH values of 7.0 and 8.0. The apparent affinity drops markedly with decreasing pH below pH 7.0, showing a slope of 1.63 on a $\log(K_{\text{app}})$ *vs.* pH plot. This is interpreted as competition between 2H^+ and Ca^{2+} for occupation of each of the two outwardly oriented translocators. The maximal values of average rate ($t = 2$ sec) and $[\text{Ca}^{2+}]_i$ were analyzed at saturating $[\text{Ca}^{2+}]_o$ values to give V_m and $[\text{Ca}^{2+}]_{i,\text{max}}$ values as a function of pH. These two parameters showed identical pH dependence, with a pH optimum between 6.0 and 6.5. These results are explained both qualitatively and quantitatively by a preliminary model of the steady-state behavior of the pump. The model assumes that enzyme dephosphorylation and countertranslocation represent the rate-limiting step of the cycle and that all other steps are at equilibrium. According to the model, the enzyme has two translocator sites, each bearing a doubly negative charge at pH 7.0 and above. Occupation of both sites by Ca^{2+} is necessary for transport. Partial or full protonation of the negative charges on the outwardly oriented translocators destroys their capacity for Ca^{2+} transport. This process is responsible for the decrease in apparent translocator affinity with decreasing pH. A $\text{p}K_a$ of 7.2 ± 0.3 was determined for the outwardly oriented translocator. Transport of 2Ca^{2+} is followed by their release to the lumen. Return of the carrier requires the loading of a charge-stoichiometric amount of alkali cation and H^+ . The pH dependence of V_m and $[\text{Ca}^{2+}]_{i,\text{max}}$ is explained by the dual effect of protonation to lower the apparent affinity of the inwardly oriented translocator for internal Ca^{2+} and to produce single and doubly protonated forms of the translocator capable of high rates of enzyme dephosphorylation and return. A $\text{p}K_a$ of 6.4 ± 0.3 was determined for the inwardly oriented form. Computer

analysis shows that the model is capable of predicting the pH dependence of the K_m , V_m and $[\text{Ca}^{2+}]_{i,\text{max}}$ values. The limitations of the model are evaluated. The structural and physiological significance of the findings is discussed.

Key Words Ca^{2+} - Mg^{2+} -ATPase · sarcoplasmic reticulum · Ca^{2+} transport · bioenergetics · ion transport · computer modeling

Introduction

Calcium uptake by the sarcoplasmic reticulum (SR) (Hasselbach & Makinose, 1963) is driven by a Ca^{2+} -dependent ATPase pump which has been the subject of a large amount of biochemical and biophysical study (MacLennan & Holland, 1975). Early work showed that two Ca^{2+} are taken up for each ATP split (Hasselbach & Makinose, 1963), and that the pump is able to reduce the external Ca^{2+} concentration to sub-millimolar concentrations (Weber, Herz & Reiss, 1966). Numerous studies (Kanazawa et al., 1971; Inesi, 1972; Froehlich & Taylor, 1975, 1976; Hasselbach, 1978; Tada, Yamamoto & Tonomura, 1978; de Meis & Vianna, 1979) have elucidated the significant reactions of the transport cycle. These include the binding of Ca^{2+} to high affinity sites of the enzyme located on the outer surface, phosphorylation of the enzyme, translocation of the occupied binding site, expulsion of the bound Ca^{2+} into the vesicle, and Mg^+ and K^+ catalyzed dephosphorylation of the enzyme, enabling the carrier to return and complete the cycle.

The present communication is concerned with the study of the Ca^{2+} -ligand interactions of the outwardly and inwardly oriented Ca^{2+} translocator, as deduced from the pH dependence of the transport K_m . Although a number of studies have reported high affinity Ca^{2+}

binding and the behavior of the Ca^{2+} K_m for transport, present knowledge does not allow us to draw conclusions about the charge of the Ca^{2+} translocator and its interaction with protons. Major findings regarding Ca^{2+} binding to the enzyme are summarized below.

Ca²⁺ Binding Studies

Ikemoto (1974) showed that the SR contains three classes of binding site. He reported a high affinity binding site with K_a values of $3.8 \times 10^6 \text{ M}^{-1}$ and $7.3 \times 10^6 \text{ M}^{-1}$ in absence and presence of ATP, respectively. The binding was studied at 0°C in a medium containing 100 mM KCl and 5 mM Mg^{2+} , at pH 7.0. Meissner (1973) reported passive Ca^{2+} binding to solubilized Ca^{2+} , Mg^{2+} -ATPase at 0°C . He showed that the affinity of the site was influenced by the Mg^{2+} concentration of the medium. At 0°C and pH 7.5 he reported K_a values of $2.6 \times 10^5 \text{ M}^{-1}$ and $1.8 \times 10^5 \text{ M}^{-1}$ for 1 mM and 5 mM Mg^{2+} , respectively. He reported the pH dependence of high affinity binding in a medium containing 100 mM KCl and 5 mM Mg^{2+} . The binding constant decreased with decreasing pH, with a maximal value of $1.3 \times 10^6 \text{ M}^{-1}$ for pH 8.1 and $0.9 \times 10^5 \text{ M}^{-1}$ for pH 6.35. In his study, and in the foregoing studies, the binding was observed to be noncooperative. Hill coefficients of 1.0 or less were reported (Meissner, 1973).

We have reported a Ca^{2+} binding constant of $5.7 \times 10^4 \text{ M}^{-1}$ for sarcoplasmic reticulum in 100 mM KCl in absence of added Mg^{2+} (Chiu & Haynes, 1977). The low value was attributed to the absence of added Mg^{2+} . Inesi et al. (1980) have reported an extensive analysis of high affinity Ca^{2+} binding to SR at pH 6.8 with 80 mM KCl and 10 mM Mg^{2+} , at 25°C . The Ca^{2+} concentrations were set using an EGTA buffer and binding was measured using the column separation techniques. Hill plots showed that the binding is cooperative with a coefficient of 1.82 and a K_a of $2.3 \times 10^6 \text{ M}^{-1}$. An overall stoichiometry of 2Ca^{2+} per phosphorylation site was observed.

Studies of K_m for Ca^{2+} Transport

A large number of studies have reported Ca^{2+} K_m values for Ca^{2+} transport and enzyme phosphorylation. Weber et al. (1966) reported half-maximal rates and uptake at $p\text{Ca}^{2+}$ values of 6.5 and 7.5, respectively. These measurements

tested the pump activity for oxalate loading at 25°C (approx. 0.8 mM, Mg^{2+} , 5 mM oxalate and pH 7). Carvalho and Leo (1967) showed half-maximal Ca^{2+} uptake at $p\text{Ca}^{2+} = 6.5$ (3.8 mM Mg^{2+} , 110 mM K^+ , pH 6.9). In these studies the maximal uptake was dependent, in part, on Ca^{2+} binding to low affinity sites of acidic binding proteins located in the SR lumen (cf. Meissner, 1975 and Chiu & Haynes, 1977). Riveiro and Vianna (1978) found cooperativity of the Ca^{2+} dependence of ATPase activity of leaky vesicles. The following values of Hill coefficient and K_{app} (reciprocal Ca^{2+} concentration for half-maximal rate) were reported for pH 7.0, $T = 30^\circ\text{C}$, 100 mM K^+ and 0.2 or 3.0 mM Mg^{2+} : $n = 1.76$ and 1.58 ; $K_{app} = 7.81 \times 10^6 \text{ M}^{-1}$ and $2.15 \times 10^6 \text{ M}^{-1}$, respectively. The former values are close to the values obtained in the present study.

Studies of K_m for Enzyme Phosphorylation

External Ca^{2+} is an absolute requirement for enzyme phosphorylation. The latter is an obligatory step in the transport cycle. Studies of the K_m of calcium activation of enzyme phosphorylation give values similar to the K_m values based on transport. Kanazawa et al. (1971) showed that the rate of enzyme phosphorylation had a second power dependence on the Ca^{2+} concentration. They reported $K_{app} (= 1/1 K_m)$ values of $(0.060 \text{ to } 1.11) \times 10^6 \text{ M}^{-1}$, the uncertainty being due to uncertainty in the Ca^{2+} -EGTA binding constant under their conditions (0°C , pH = 7.0). Yamada and Tonomura (1972) performed the same measurements on deoxycholate-solubilized SR and reported $K_{app} = 2.9 \times 10^6 \text{ M}^{-1}$ and a Hill coefficient of 2.0 for pH 7.0, $T = 0^\circ\text{C}$. Verjovski-Almeida and de Meis (1977) studied the K_m for Ca^{2+} -induced increase in phosphoenzyme level at 30°C with leaky vesicles. Figure 3 of their paper indicates the following K_{app} values as a function of pH: $10^{4.8}$, pH 6.1; $10^{6.0}$, pH 7; $10^{8.5}$, pH 8.65. They reported a further increase in phosphoenzyme level correlated with Ca^{2+} -occupation of the inwardly oriented form of the translocator. These K_{app} values (reciprocal of $[\text{Ca}^{2+}]_i$ for half-maximal inhibition) were shown to vary between $0.62 \times 10^3 \text{ M}^{-1}$ and $1 \times 10^4 \text{ M}^{-1}$ for pH 7.0 and 8.3, respectively. The pH 7 value is close to the inhibitory constant which can be calculated from the kinetic data on phosphoenzyme decay at 0°C presented by Yamada and Tonomura (1972). Reports of the pH depen-

dence of the high affinity binding site (Yamada & Tonomura, 1972; Meissner, 1973) suggested to us that the translocator bears titratable groups and motivated the present study.

The present communication reports the pH dependence of the average rate, maximal steady-state Ca²⁺ uptake, their K_{app} values with respect to Ca²⁺, and the gradient achieved by the pump at half-saturation. This is accomplished by measuring the progress curve of active uptake at a number of EGTA-buffered Ca²⁺ concentrations over a range of pH values. Such studies have been made possible for the rapid and continuous monitoring of the free internal Ca²⁺ concentration achieved by the pump (Chiu et al., 1980; Chiu & Haynes, 1980a, b).

Materials and Methods

Sarcoplasmic Reticulum

The low density Ca²⁺, Mg²⁺-ATPase-rich fraction of rabbit skeletal sarcoplasmic reticulum (SR) was prepared by density gradient centrifugation as described previously (Chiu et al., 1980). Sodium dodecylsulfate (SDS) gel electrophoresis showed that over 90% of the total protein is ATPase, and that the fraction is essentially devoid of acidic binding proteins.

Instrumentation

Stopped-flow experiments were carried out with an Aminco-Morrow Stopped-Flow Apparatus (Catalog no. 4-8409). The apparatus mixes equal volumes of two solutions. The excitation monochromator was set at 368 nm and a Schott GG420 cut-off filter was placed in front of the photomultiplier. On-line data acquisition was performed using a Digital Equipment Corporation 1103 computer. Analog-digital conversion was performed after activation of our stopped-flow program by the trigger impulse from the stopped-flow spectrometer. Rapid sampling (1000 Hz) was performed during the first 100 msec, followed by 25 Hz for the first 2 sec and 5 Hz for the remainder of the reaction. The fluorescence *vs.* time progress curves were stored on floppy discs and analyzed subsequently. SR was pre-equilibrated in a medium with a Ca²⁺/EGTA buffer and active transport was initiated by a Mg-ATP jump. The free Ca²⁺ concentration was set by adjustment of the Ca²⁺/EGTA ratio. The final media were checked for correctness of pH before the experiment was performed. Solutions were made from doubly distilled and deionized water, and special care was taken to avoid Ca²⁺ contamination. Possible influence of contamination on the free Ca²⁺ concentration was checked by repetition of the experiment with twice the normal EGTA concentration at constant Ca²⁺/EGTA ratio. The finding of identical results in the two experiments indicates the absence of contaminating Ca²⁺. The free external Ca²⁺ concentration [Ca²⁺]_o was calculated from the Ca²⁺ to EGTA ratio

Table 1. Apparent Ca²⁺-EGTA binding constant (K_a) as a function of pH

pH	K_a (M ⁻¹)	pH	K_a (M ⁻¹)
5.5	4.075×10^3	7.0	3.774×10^6
6.0	3.909×10^4	7.5	3.672×10^7
6.5	3.832×10^5	8.0	3.087×10^8

with the help of a computer program using the EGTA complexation and association constants tabulated by Fabiato and Fabiato (1978) and Martell and Smith (1974), corrected for temperature using the ΔH values given in the latter reference. The apparent Ca²⁺-EGTA binding constants are given as a function of pH in Table 1.

A series of active uptake experiments were performed at a number of Ca²⁺/EGTA ratios. Under identical conditions and on the same day, a number of Ca²⁺ jump experiments were performed in absence of EGTA and ATP. These served as passive calibrations of the fluorescence *vs.* free internal calcium concentration dependence. The active transport fluorescence *vs.* time data were transformed by the data obtained in passive equilibration experiments as described in the Results section. The average rate was determined for the first 2 sec of reaction. Although the average rate was significantly lower than the rate observed during the first 100 msec, it was more accurately determined and was considered to be more representative of the behavior of the enzyme at steady state.

Significant Experimental Conditions Relating to Interpretation

As has been noted previously (Chiu & Haynes, 1980b; Haynes, 1982) the light fraction of ATPase-rich SR consists of two types of vesicle with respect to K⁺ permeability (McKinley & Meissner, 1977, 1978). Type I contains channels for monovalent cations and anions, and is thus KCl permeable. Type II contains neither type of channel and is KCl impermeable. We have shown previously (Chiu & Haynes, 1980a) that Type II vesicles can be made KCl permeable by the addition of valinomycin to a final concentration of approximately 6×10^{-6} M. Valinomycin addition serves to unmask the activity of the pump in Type II vesicles (Chiu & Haynes, 1980b; Haynes, 1981). The reader is referred to these papers for a more detailed description of these findings. We have shown that pH imbalances can occur across the SR membrane in the absence of a penetrating buffer (Haynes, 1982). To ensure that the internal and external pH are equal, we have included 20 mM Tris in the medium. The ATP concentration was kept at less than optimal concentration (1×10^{-4} M). This was done in order that enzyme dephosphorylation and subsequent return of the carrier will constitute a rate-limiting step in the transport cycle, thereby simplifying the analyses. The medium contained 0.6 M sucrose. This has been shown to permeate the membrane at a moderate rate ($t_{1/2}$ approximately 5 min). Our SR was preincubated in the medium for at least this amount of time. Thus the high concentration of sucrose allows it to work as an osmotic buffer to allow for maximal Ca²⁺ uptake to occur without exposing the membrane to osmotic strain. In summary, the conditions were adequate for ATP-supported Ca²⁺ uptake by both types of SR, and

the net transport occurs as CaCl_2 accumulation. The active transport amplitudes were found to be independent of the preincubation times for all pH values except 5.5. At this pH, the amplitude was observed to decrease as a function of time that the sample was in the apparatus. The data presented for pH 5.5 were taken after approximately 1 min exposure, the minimal time for sample preparation and loading.

Data Acquisition and Analysis

Active uptake was studied as a function of both external Ca^{2+} concentration and pH. The data set for the present publication consists of over 600 progress curves. One week of experimentation was necessary to generate a complete set of fluorescence *vs.* time progress curves and their calibrations. The data were stored on floppy disks and were subsequently converted into Ca^{2+} *vs.* time curves. The latter were analyzed for average rate for the first 2 sec of the reaction and for steady-state maximal uptake. These data were analyzed, in turn, for pH dependence of K_{app} and V_m . This data acquisition cycle was repeated three times to generate the data set of the present paper. Thus, K_{app} , V_m and steady-state maximal uptake values are the average of at least three separate experiments with three separate preparations. The progress curves for any particular experiment with any particular preparation were highly reproducible and showed low noise levels (less than 5%). Thus the progress curves shown here are the result of a particular experiment rather than the average of several. Plots of K_{app} *vs.* pH and K_{app} velocity *vs.* pH were generated by our computer programs KAPP and EQMOD, respectively, under the experimental conditions and using $[\text{Ca}^{2+}]_i = 3 \text{ mM}$ appropriate for averaging of the average rates over the first 2 sec. The programs use the model described in the Appendix to calculate K_{app} or initial velocity as a function of pH (3 or 4 points between minimal and maximal pH values) using the experimental values of the concentrations of K^+ and internal and external Ca^{2+} . The values of the equilibrium and kinetic constants are set by the operator, and the program has the option of looping back to make systematic adjustments in one or more of the constants and to compare the calculated curve with the previous results. A description of our procedure for conforming the model to the data is given in the text.

Results

Figure 1 shows the response of ANS^- fluorescence to active Ca^{2+} transport initiated by rapid mixing of ATP with Ca^{2+} , Mg^{2+} -ATPase-rich fraction of the sarcoplasmic reticulum (SR). Previous work (Chiu *et al.*, 1980; Chiu & Haynes, 1980*a, b*) has shown that this is the net result of an increase in internal free Ca^{2+} concentration ($[\text{Ca}^{2+}]_i$) resulting from transport. Figure 2 is a calibration curve giving the dependence of the increase in fluorescence on the internal free Ca^{2+} concentration. The curve was determined by performing Ca^{2+} jump experiments in the absence of ATP. The data of Fig. 1 were transformed by Fig. 2 to produce

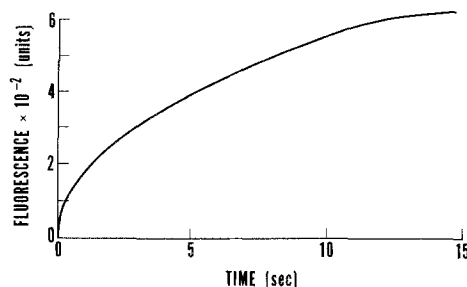


Fig. 1. Typical progress curve of Ca^{2+} -transport-induced ANS^- fluorescence increase. ANS^- fluorescence was measured in an Aminco-Morrow stopped-flow apparatus as described previously (Chiu & Haynes, 1980*b*). The medium consisted of 0.6 M sucrose, 100 mM KCl, 1×10^{-4} M MgCl_2 , 20 mM Tris and 10 mM Hepes buffer, pH 7, a Ca^{2+} /EGTA buffer (total EGTA = 1 mM, Ca^{2+} /EGTA ratio = 0.17), and 1×10^{-5} M ANS . Syringe A contained 0.1 mg/ml SR and 6×10^{-6} M valinomycin. Syringe B contained 1 mM Mg ATP. The reaction was studied at 30°C. The calculated free external Ca^{2+} concentration was 5.4×10^{-8} M

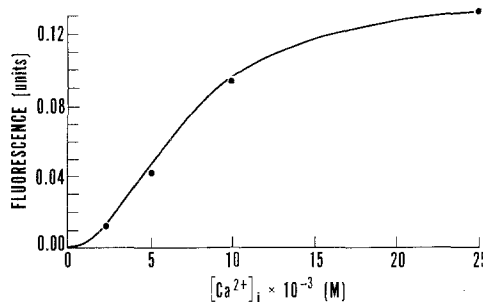


Fig. 2. Typical calibration graph of fluorescence increase *vs.* free internal Ca^{2+} concentration. The results were obtained on the same day as the results of Fig. 1. The response of ANS^- fluorescence (Y-axis) to an increase in internal free Ca^{2+} concentration from 0 to 25 mM was obtained as the total amplitude resolved by the stopped-flow spectrometer ($t = 3 \text{ msec}$ to 500 sec after mixing) to jumps in Ca^{2+} concentration to the indicated values. Further details have been given previously (Chiu & Haynes, 1980*b*). The medium and reaction conditions were identical to those of Fig. 1 except that Ca^{2+} /EGTA and Mg -ATP were omitted. The X-axis represents the Ca^{2+} concentration after the jump. The solid line represents a computer fit of the data according to $F = \frac{[(x(1) * ([\text{Ca}]^{**} x(3)))]}{[1 + (x(1) * ([\text{Ca}]^{**} x(3)))]} * x(2)$ where * represents multiplication and ** represents exponentiation. The fitted values were as follows: $x(1) = 1.396 \times 10^2$, $x(2) = 0.1383$, $x(3) = 2.233$. The fit was performed as an aid to data processing; no theoretical significance is attached to the values of the fitted constants

the progress curve of Ca^{2+} transport shown in Fig. 3. The free internal Ca^{2+} concentration increases to 6.35 mM in *ca.* 15 sec, with half-time of 1.0 sec. The internal Ca^{2+} concentration is seen to rise rapidly in the first second, followed by subsequent increase at continuously decreas-

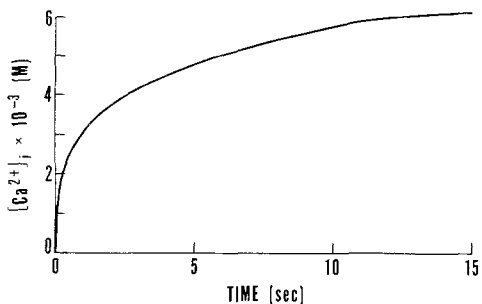


Fig. 3. Progress curve of ATP-energized Ca^{2+} uptake. The data of Fig. 1 are transformed into internal free Ca^{2+} concentration using the equation and constants used to fit the calibration curve of Fig. 2

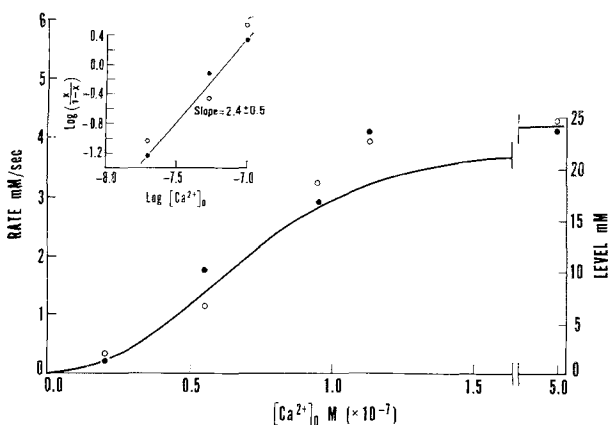


Fig. 4. Ca^{2+} concentration dependence of average rate ($t = 2$ sec) and maximal steady-state level at pH 7.0. Experiments of Figs. 1 and 3 were repeated at a number of Ca^{2+} /EGTA ratios and the corresponding $[\text{Ca}^{2+}]_o$ values were calculated as described in Materials and Methods. Rates, determined at $t = 2$ sec, are denoted by solid circles; maximal steady-state levels are denoted by open circles. The maximal steady-state level at saturating $[\text{Ca}^{2+}]_o$ will be referred to as $[\text{Ca}^{2+}]_{i,\text{max}}$. The Figure presents the data for one of three sets of experiments done at pH 7.0. The solid line is for y values plotted as $y/y_{\text{max}} = (K_{\text{app}}[\text{Ca}]_o)^{2.4} / (1 + (K_{\text{app}}[\text{Ca}]_o)^{2.4})$ with $K_{\text{app}} = 1.37 \times 10^7 \text{ M}^{-1}$

ing rates, until the steady-state maximal uptake is achieved. In our studies of the transport rate as a function of $[\text{Ca}^{2+}]_o$ and pH, we have taken the $[\text{Ca}^{2+}]_i$ calculated at $t = 2$ sec as the measure of the average rate. This was necessary because rates measured at shorter times were of lesser accuracy, particularly at low $[\text{Ca}^{2+}]_o$ and pH values which give low fluorescence amplitudes.

The experiment of Fig. 3 was repeated at a number of Ca^{2+} /EGTA ratios and the average rates were evaluated at $t = 2$ sec. Figure 4 is the result of a typical experiment showing the average rates and steady-state maximal uptakes

plotted against the free Ca^{2+} concentration of the medium. The latter quantity was calculated from the Ca^{2+} -EGTA ratio as described in Materials and Methods. The plot shows a "sigmoidal" dependence of both the average rate ($t = 2$ sec) and maximal steady-state level on the free external Ca^{2+} concentration. Half-maximal rates and uptakes were observed at $7.3 \times 10^{-8} \text{ M}$ external Ca^{2+} . The insert is a Hill plot of the same data. A slope of 2.4 ± 0.5 was measured for both of these parameters. Repetition of the experiment at other pH values showed that the cooperativity diminishes, with decreasing pH below 7.0. A first-order power dependence was observed at pH 5.5. Our results at pH 7 indicate an apparent affinity constant, $K_{\text{app}} (= 1/K_m) = 1.37 \times 10^7$. The solid line is a theoretical curve calculated using this constant and a 2.4-power dependence on $[\text{Ca}^{2+}]_o$. A reasonable fit of the data is obtained. The value of K_{app} is in fair agreement with the value reported by Riviero and Vianna (1978) for ATPase activity of leaky vesicles ($7.81 \times 10^6 \text{ M}^{-1}$ for 0.2 mM Mg^{2+}) and on the Ca^{2+} -dependence of enzyme phosphorylation reported by Kanazawa et al. (1971).

The experiments of Figs. 1-4 were repeated at a number of pH values ranging from 5.5 to 8.0. The values of K_{app} and the maximal values of average rate and maximal steady-state uptake were determined. The latter will be referred to as $[\text{Ca}^{2+}]_{i,\text{max}}$. Within any particular series of experiments at a given pH, the K_{app} values for rate and steady-state maximal uptake were indistinguishable. The experimental uncertainty in their measurement was about 10%. This indicates that the average rate and maximal steady-state uptake share the same dependence on external Ca^{2+} concentration. The K_{app} value showed only small variation from one day to the next and from one preparation to another. The maximal values of average rate and steady-state uptake showed considerable variation.

Figure 5 shows the dependence of K_{app} on pH. The average values of $\log(K_{\text{app}})$ from three series of experiments with three preparations are plotted against pH. A three order of magnitude variation of K_{app} is observed over the 5.5 to 8.0 pH range. The Figure shows that the data can be reasonably well fit by two straight-line segments. In the range of pH 7.0 to 8.0, a relatively small dependence is observed with a slope of 0.38. In the low pH range (5.5 to 7.0) a greater dependence is observed with a slope of 1.63. In the Discussion section we will show

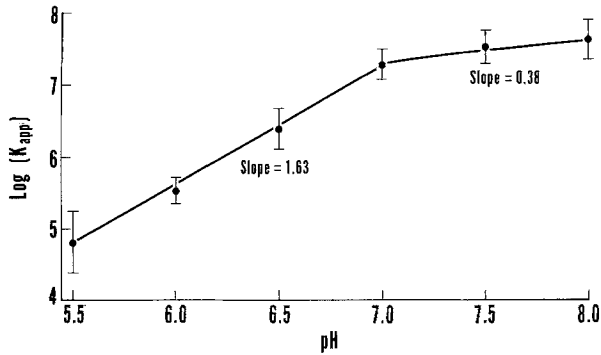


Fig. 5. The pH dependence of K_{app} . The experiment of Fig. 4 was carried out at the indicated pH values. The data are the average of three sets of experiments. The error bars indicate \pm SD between experiments

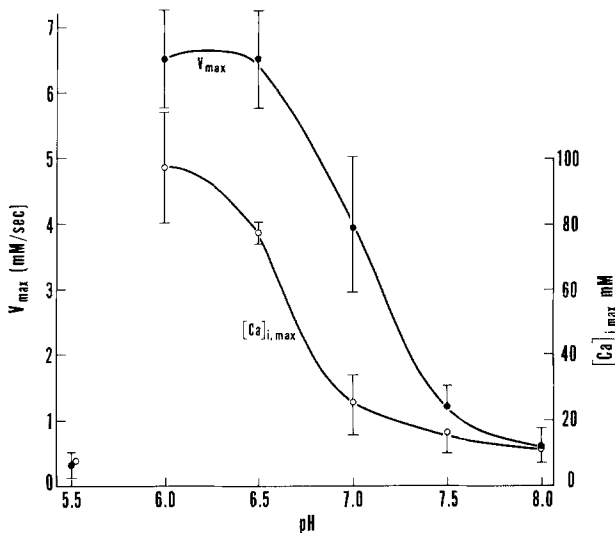


Fig. 6. The pH dependence of the maximal values of average rate ($t=2$ sec) and $[\text{Ca}^{2+}]_i$ at steady state. The data are the average of three sets of experiments. The error bars indicate \pm SD between experiments

that the 1.63 power dependence of K_{app} on the H^+ concentration can be approximated by an extremely simple model. According to the model, 1-4 H^+ compete with 2 Ca^{2+} for occupation of the two outwardly oriented translocators.

Figure 6 shows the pH dependence of the maximal value of the average rate at saturating external Ca^{2+} concentrations (V_{max}) and of the steady-state maximal Ca^{2+} uptake ($[\text{Ca}^{2+}]_{i,max}$). The results are the average of three series of experiments with three preparations. The standard deviations reflect variation in the maximal rate from preparation to preparation. The shape of the curve did not vary between preparations. Optimal values of V_{max} and $[\text{Ca}^{2+}]_{i,max}$ were observed at pH 6.0 to 6.5.

The rates and the maximal uptakes fall off rapidly between pH 6.0 and 5.5. This was in part due to irreversible loss of transport function, since active uptake amplitudes were observed to decrease with time of preincubation at pH 5.5, as discussed below.

Berman, McIntosh and Kench (1977) have shown that the Ca^{2+} uptake, but not the Ca^{2+} -ATPase function, is irreversibly inactivated by incubation at pH 5.5. The $t_{1/2}$ for inactivation at 37°C was of the order of 1 min, the minimal preincubation time in our experiments. This is the time necessary for loading the sample into the apparatus. Active uptake amplitudes were observed to decrease as a function of time of incubation in the apparatus, in a manner consistent with irreversible inactivation, but it was not possible to study the kinetics of the process due to the low degrees of uptake and the low sensitivity of the method at pH 5.5. It is therefore probable that our low V_m measured at pH 5.5 reflects irreversible inactivation and that average rates of two to several times the presented values would have been observed if it had been possible to measure average rates with zero preincubation time.

In contrast, the rates and amplitudes observed between pH 6.0 and 8.0 were independent of preincubation time and are thus considered true measures of the steady-state behavior of the enzyme. The V_m and $[\text{Ca}^{2+}]_{i,max}$ values were maximal at pH 6.0 and 6.5 and dropped off sharply with increasing pH between 6.5 and 8.0. In the Discussion section, we will present a model which explains this effect in terms of $\text{H}^+/\text{Ca}^{2+}$ competition for occupation of the inwardly oriented translocator.

The ability of the Ca^{2+} - Mg^{2+} -ATPase pump to produce and maintain a gradient is of physiological and bioenergetic interest. We have previously reported gradients of 2.8×10^3 under conditions of saturation with external Ca^{2+} and maximal pump activation (Chiu & Haynes, 1980b). The present study has demonstrated to us that these are not optimal conditions for establishment of a maximal gradient. Figure 7 shows the pH dependence of the Ca^{2+} gradient measured at $[\text{Ca}^{2+}]_o = K_m$, as a function of pH. Concentration gradients of the order of 10^5 are observed over a broad range of pH (6.5 to 8.0), indicating tight coupling between ATP hydrolysis and Ca^{2+} movement (cf. Dixon, Corbett & Haynes, 1982). Below pH 6.5, the ability of the pump to maintain a gradient decreases with decreasing pH.

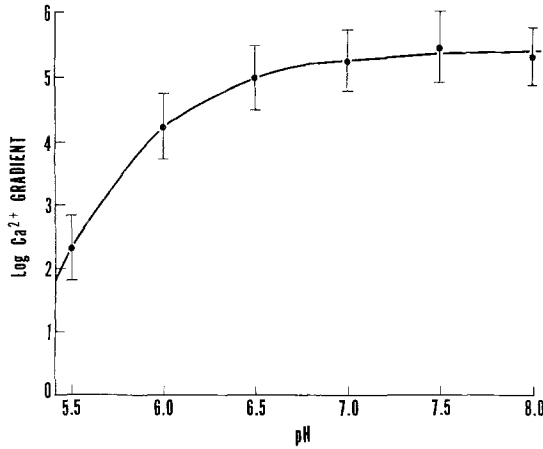


Fig. 7. The pH dependence of the $[\text{Ca}^{2+}]_i/[\text{Ca}^{2+}]_o$ ratio at steady state, evaluated at $[\text{Ca}^{2+}]_o = K_m$

Discussion

The present communication has reported the pH and Ca^{2+} concentration dependence of the Ca^{2+} , Mg^{2+} -ATPase pump. Progress curves were obtained at variable external Ca^{2+} concentrations and pH values, and the V_m and $K_{app}(=1/K_m)$ values for the average rate ($t = 2$ sec) and maximum uptake at steady state were presented. The K_{app} values are maximal at high pH, decreasing sharply with decreasing pH for values below 7.0. The V_m increases from pH 7.0 to 6.5, shows optimal values between pH 6.5 and 6.0. At pH 5.5, much lower V_m values are observed, but this is in part due to irreversible inactivation. Thus decreasing the pH in the range 8.0 to 6.0 has the opposite effects of decreasing the apparent affinity of the pump but increasing the maximal rate of transport. In the remainder of this communication we will consider a model which explains these effects.

Model Involving Translocator Protonation

We have tested a large number of models, using different assumptions about the numbers of Ca^{2+} , K^+ and H^+ bound and the position of the rate-limiting step in the transport cycle. Figure 8 presents the simplest model which we have found capable of predicting the aforementioned pH dependencies of K_{app} and V_m and $[\text{Ca}^{2+}]_{i,max}$. The model incorporates the major mechanistic features demonstrated by others (Kanazawa et al., 1971; Froehlich & Taylor, 1975, 1976; Inesi et al., 1978a,b; Noack et al., 1978) and our findings (Chiu & Haynes, 1980b)

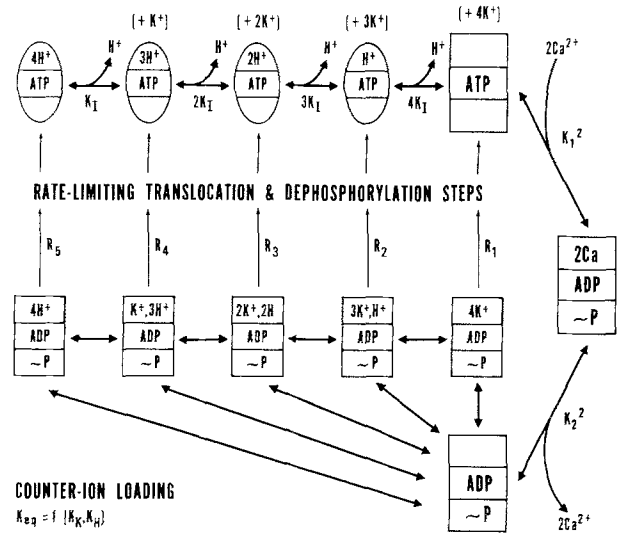
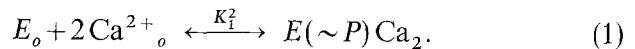
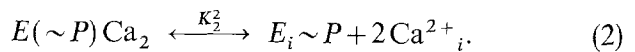


Fig. 8. Model for Ca^{2+} , Mg^{2+} -ATPase function. The model is applicable to the present experimental conditions: saturating Mg -ATP concentrations, and low phosphate, ADP, and free Mg^{2+} concentrations. ATP and ADP denote the Mg^{2+} complexes

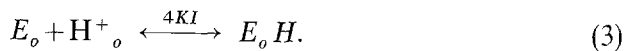
that internal K^+ is necessary for maximal rates of transport. In the first step of the transport sequence the two outwardly oriented translocators are loaded and the enzyme is phosphorylated according to:



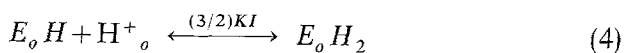
The two translocators change to inward orientation and release 2Ca^{2+} to the interior:



According to the model, the affinity of the carrier is modulated by H^+ binding to the outwardly oriented translocators and by H^+ and K^+ binding to the inwardly oriented translocators. The first step of H^+ binding to the outwardly oriented form is:

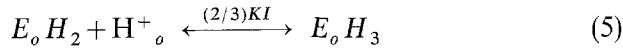


This serves to inhibit Ca^{2+} transport by competition. The reaction has an intrinsic constant of KI , with the factor of 4 to account for 4 binding sites (see Appendix). Further binding occurs by:

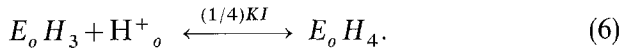


where the factor 3/2 accounts for the fact that the $E_o H_2$ can be formed by binding to any of the three open binding sites while the complex

can be broken down by association of either of the two H -occupied sites (*see* Appendix). Similarly the binding to the two remaining sites occurs by:



and:



The model assumes that both H^+ and K^+ can bind to the inwardly oriented translocator, with intrinsic binding constants KH and KK , statistically weighted in a similar manner (*see* Appendix). These binding reactions stimulate transport by facilitating the return of the carrier (Chiu & Haynes, 1980*b*). The model further assumes that dephosphorylation and countertransport of the five fully K^+ - and H^+ -laden forms represent rate-limiting steps in the transport cycle. All other reactions are assumed to be at equilibrium. This assumption is not correct for the first approximate 200 msec of the reaction, and thus average rates were not analyzed in that time region. Instead the average rate was calculated at $t=2$ sec. We realize that the assumptions of the model may not be correct under all experimental conditions of this study, but we consider the simplification made in this model to be necessary for preliminary quantitative consideration of the data.

The rate constants for the rate-limiting dephosphorylation and countertransport reactions are defined as R_1, \dots, R_5 for the fully laden EK_4, \dots, EH_4 forms, respectively. They are expressed as the rate of increase in the internal Ca²⁺ concentration (M/liter sec), but can also be thought of as the turnover number of the enzyme times the number of translocator sites divided by the luminal volume. Thus the overall rate of transport (Rate) will be given as:

$$\text{Rate} = \frac{R_1 [E_i K_4] + R_2 [E_i K_3 H] + R_3 [E_i K_2 H_2] + R_4 [E_i K H_3] + R_5 [E_i H_4]}{[E]_i} \quad (7)$$

where E_i represents the total enzyme. The development in the Appendix shows that the model predicts the following dependence of the enzyme rate on cation concentrations:

$$\text{Rate} = \frac{(F1-KK-KH)(K_1 [Ca]_o)^2}{(F-KI)([Ca]_i^2/K_2^2)} \frac{1}{((F2-KK-KH) + ([Ca]_i^2/K_2^2))(K_1 [Ca]_o)^2 + 1} \quad (8)$$

where $F1-KK-KH$ is a function expressing the contributions of the fully laden, inwardly oriented forms of the translocator:

$$(F1-KK-KH) = (R_1 (KK [K]_i)^4 + 4R_2 (KK [K]_i)^3 (KH [H]_i) + 6R_3 (KK [K]_i)^2 (KH [H]_i)^2 + 4R_4 (KK [K]_i) (KH [H]_i)^3 + R_5 (KH [H]_i)^4) \quad (9)$$

and where $F2-KK-KH$ is a function giving the relative weights of the partially and fully laden forms of the inwardly oriented translocator:

$$(F2-KK-KH) = (1 + 4K(1 + (3/2)K)(1 + (2/3)K(1 + K/4))) + 4H(1 + 3K(1 + K(1 + K/3))) + 6H^2((1 + 2K(1 + K/2)) + 2/3H(1 + H/4) + K) \quad (10)$$

with K representing $KK [K^+]_i$ and H representing $KH [H^+]_i$. The function $(F-KI)$ expresses the inhibitory effect of protonation of the outwardly oriented translocator. Its value is given by:

$$(F-KI) = 1 + 4KI[H]_o + 6(KI[H]_o)^2 + 4(KI[H]_o)^3 + (KI[H]_o)^4. \quad (11)$$

Although Eq. (8) would seem to be complex, it involves only five adjustable equilibrium constants (K_1, K_2, KI, KH and KK) and five rate constants (R_1, \dots, R_5) for the return of the variously laden forms of the carrier. Our experience has shown that the model can fit the data with a very limited range of rate and equilibrium constant values.

pH Dependence of K_{app}

Equation (8) predicts a second power dependence of the average rate on $[Ca^{2+}]_o$ as observed (Fig. 5). The value of K_{app} is given as:

$$K_{app} = K_1 \left(\frac{(F2-KK-KH) + ([Ca]_i^2/K_2^2)}{(F-KI)([Ca]_i^2/K_2^2)} \right)^{1/2}. \quad (12)$$

The $(F-KI)$ term in the denominator involving $[H^+]_o$ gives rise to a decrease in apparent

Ca^{2+} affinity due to protonation of the outwardly oriented translocator. This effect is countered by the effects of protonation of the inwardly oriented carrier which causes the F_2 - KK - KH term in the numerator to increase with decreasing pH. For the case $\text{KH} < \text{KI}$, and for $\text{KK}[\text{K}^+] > 1$, the pH dependence of K_{app} is governed by F - KI term in the denominator. Figure 9 compares the pH dependence observed for K_{app} with that calculated according to Eq. (12), with the constants given in the Figure legend. The K_1 value is made equal to the apparent Ca^{2+} affinity ($2.3 \times 10^6 \text{ M}^{-1}$) of the pump in absence of ATP at pH 6.8 reported by Inesi et al. (1980). The value of K_2 is close to the values of the inhibitory constant of Ca^{2+} on enzyme dephosphorylation reported by others (Kanazawa et al., 1971; Verjovski-Almeida & de Meis, 1977; Inesi et al., 1978a,b). The KK value of 30 M^{-1} was chosen to make the calculated K_{app} value agree with $1/K_m$ value for Ca^{2+} . It is in fair agreement with K^+ concentration dependence of the rate of transport at pH 7.0 (Chiu & Haynes, 1980b) and with the reciprocal of the K_m value (20.8 M^{-1}) reported by Shigekawa and Dougherty (1978) for K^+ catalysis of $E \sim P$ decomposition. The Figure shows fits of the data for three values of KH . The fit is quite sensitive to the KI value over the whole pH range and is sensitive to the KH value at low pH. The next section will show that the fit of the V_m vs. pH data is extremely sensitive to the choice of KH . Figure 9 shows good agreement between theory and experiment. The intrinsic pK_a value of 7.2 is thus determined for the outwardly oriented form of the translocator using $\text{pK}_a = -\log(\text{KI})$.

pH Dependence of V_m

Figure 10 shows the calculation of V_m vs. pH for saturating external Ca^{2+} concentrations (1 mM) and for the values of the constants used in Fig. 9. The three calculated curves use the KH values corresponding to the curves of Fig. 9. The dotted curves are calculated from the same constants using higher values of the counter-translocation rate constants for the more highly protonated species. This was attempted since the true V_m values at pH 5.5 were probably underestimated in our study. In any case the fit of the data for pH 6.0 to 8.0 is sensitive to the KH value chosen. A value of $\text{KH} = 2.5 \times 10^6 \text{ M}^{-1}$ gives the best agreement for the data of Fig. 10. This value corresponds to a pK_a of

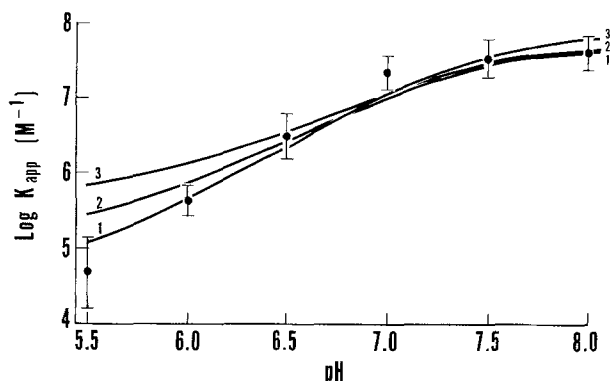


Fig. 9. pH dependence of K_{app} . Computer program K_{APP} was used for calculations. $K_1 = 2.3 \times 10^6 \text{ M}^{-1}$, $\text{KK} = 3.0 \times 10^6 \text{ M}^{-1}$, $\text{KI} = 1.5 \times 10^7 \text{ M}^{-1}$, $K_2 = 5.4 \times 10^{-3} \text{ M}$, $\text{pH} = \text{pH}_o$, 0.1 M K^+ , $[\text{Ca}^{2+}]_i = 3 \text{ mM}$. Curve 1: $\text{KH} = 1.25 \times 10^6 \text{ M}^{-1}$; Curve 2: $\text{KH} = 2.5 \times 10^6 \text{ M}^{-1}$; Curve 3: $\text{KH} = 5.0 \times 10^6 \text{ M}^{-1}$. Points are from Fig. 5

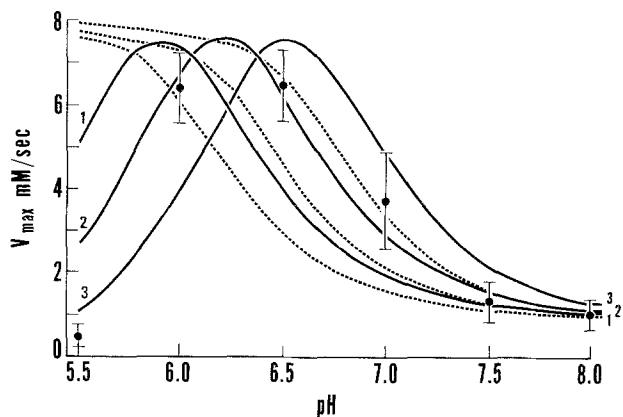


Fig. 10. Calculation of pH dependence of V_m . The computer program EQMOD was used. The constants were fitted as in Fig. 9 with $[\text{Ca}^{2+}]_o = 1 \text{ mM}$, $[\text{Ca}^{2+}]_i = 3 \text{ mM}$. The following rate constants were assigned for the various fully laden inwardly oriented forms of the translocator: $EK_4 = 3.0 \times 10^{-4} \text{ M/sec}$, $EHK_3 = 1.69 \times 10^{-2} \text{ M/sec}$, $EH_2K_2 = 8.43 \times 10^{-3} \text{ M/sec}$, $EH_3K = 7.0 \times 10^{-5} \text{ M/sec}$, $EH_4 = 7.0 \times 10^{-5} \text{ M/sec}$. Curves 1-3 are calculations for $\text{KH} = 1.25 \times 10^6 \text{ M}^{-1}$, $\text{KH} = 2.5 \times 10^6 \text{ M}^{-1}$, $\text{KH} = 5.0 \times 10^6 \text{ M}^{-1}$, respectively. The dotted lines give the corresponding curves for $EK_4 = 3.0 \times 10^{-3} \text{ M/sec}$, $EHK_3 = 9.5 \times 10^{-3} \text{ M/sec}$, $EH_2K_2 = 9.5 \times 10^{-3} \text{ M/sec}$, $EH_3K = 9.5 \times 10^{-3} \text{ M/sec}$, $EH_4 = 9.5 \times 10^3 \text{ M/sec}$

6.4 for the inwardly oriented translocators. The value fits all data in Fig. 9 within the experimental error except for the $\text{pH} = 5.5$ point. In order to simulate the pH dependence between pH 8.0 and 6.5 the rate constants for dephosphorylation and translocation of E_iHK_3 and $E_iH_2K_2$ must be larger than for E_iH_4 . Their respective values for the best fit are 16.7, 8.4 and 3.0 mM/sec . Since the V_m at pH 5.5 is poorly defined, the rate constants for the E_iKH_3 and the E_iH_4 forms are not defined.

Table 2. Analysis of best fit values and their maximal error

Constant	Value	Maximal range of variation	Comment
K_1	$2.3 \times 10^6 \text{ M}^{-1}$	$(1-5) \times 10^6 \text{ M}^{-1}$	Taken from Inesi et al. (1980). Can be fitted by maximal value of K_{app} . Maximal variation is sensitive to values of K_2 and KK
K_2	$5.4 \times 10^{-3} \text{ M}$	$(2.2-7.7) \times 10^{-3} \text{ M}$	The shape of the initial portions of the $[\text{Ca}^{2+}]$ vs. time curve are very sensitive to this constant
KK	$3.0 \times 10^1 \text{ M}^{-1}$	$(1-6) \times 10^1 \text{ M}^{-1}$	Determined by saturability of initial rate with respect to $[\text{K}^+]$. Overestimation underestimation results in poor fit of Fig. 10. Its value is interactive with K_1
KI	$1.5 \times 10^7 \text{ M}^{-1}$	$(0.8-3.0) \times 10^7 \text{ M}^{-1}$	The fit of the shape of Fig. 9 is very sensitive to this parameter
KH	$2.5 \times 10^6 \text{ M}^{-1}$	$(1.5-5.0) \times 10^6 \text{ M}^{-1}$	The values of this parameter are very closely defined by the requirement for fitting the data of Fig. 9 and Fig. 10
$R_1(EK_4)$	$3.00 \times 10^{-3} \text{ M/sec}$	$(1.0-4.0) \times 10^{-3} \text{ M/sec}$	Well defined from high pH data of Fig. 10
$R_2(EHK_3)$	$1.69 \times 10^{-2} \text{ M/sec}$	$(0.7-2.0) \times 10^{-2} \text{ M/sec}$	Defined by maximum of Fig. 10
$R_3(EH_2K_2)$	$8.4 \times 10^{-3} \text{ M/sec}$	$(6-10) \times 10^{-3} \text{ M/sec}$	Defined by maximum of Fig. 10 Somewhat interactive with KH
$R_4(EH_3K)$	-	-	Poorly defined
$R_5(EH_4)$	-	-	Poorly defined

The effects of pH on Mg-ATP binding are without influence in our experiments since the Mg-ATP concentration is over an order of magnitude higher than the K_m and since Meissner (1973) has reported less than fourfold variation in the K_m from pH 6 to 9. It is interesting that Masuda and de Meis (1973) reported a pH dependence for enzyme phosphorylation ("low energy") by high $\text{Mg}^{2+} + \text{Pi}$ which is similar to our pH profile of V_m . Although our experimental conditions could not produce appreciable amounts of low energy phosphoenzyme, the similarity of the two phenomena may indicate that they have steps in common.

The present analysis was based on the assumption that the pH effects were expressed through occupation of the translocator sites. It reproduces the affinity data over a nearly three-order of magnitude variation in apparent affinity and reproduces the pH dependence of the V_m using the same constants. We consider the model to be a very good approximation of the significant interactions of the enzyme with internal and external Ca^{2+} and H^+ . All of the constants used in the fit were varied systematically to test the accuracy with which they were determined. Table 2 gives the best value of the constants, and their maximal range of variation. The latter was judged by the criterion of good-

ness of fit of the data of Figs. 9 and 10 upon perturbation of the constant to be tested. Mutual cancellation of the effects of the perturbations of the constants was also taken into consideration. The pK_a value of the outwardly oriented translocators (pK_I) is determined as 7.2 ± 0.3 . The pK_a value of the inwardly oriented translocator is shown to have a lower value of 6.4 ± 0.3 . It is determined in a more model-dependent fashion and is thus less accurately determined. We also conclude that the rate constants for dephosphorylation and translocation of the $E_iH_2K_2$ and E_oHK_3 forms are higher than that of the E_iK_4 form. The exact ratios are not well defined by the curve fitting.

Inhibition of Uptake by Internal Ca^{2+}

We have presented calculations showing that a single pump turnover releasing 2Ca^{2+} per pump will raise the internal Ca^{2+} concentration to as much as 15 mM if the Ca^{2+} could be completely dissociated from the inwardly oriented translocator (Chiu & Haynes, 1980b). The ATPase-rich SR fraction does not contain an appreciable amount of low affinity Ca^{2+} -binding proteins, and at pH 7 the pump is thus inhibited by the translocated Ca^{2+} before the first cycle is completed (Chiu &

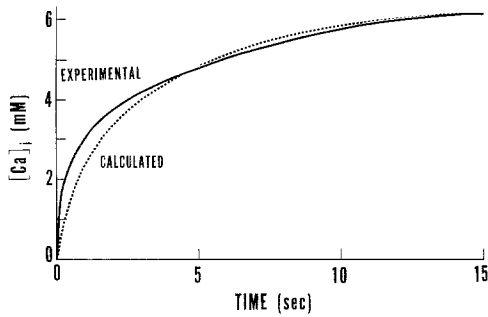


Fig. 11. Comparison of an actual and calculated progress curve. The experimental conditions were identical to Fig. 3. The progress curve was calculated using Eq. (13), the constants of Fig. 10 ($KH=2.5 \times 10^6 \text{ M}^{-1}$), $k_{\text{leak}}=4.8 \times 10^{-2} \text{ sec}^{-1}$ and with the R values corresponding to the solid lines in Fig. 10

Haynes, 1980*b*). We have used Eq. (8) to analyze the progress curves of the uptake reaction as a means of establishing the value of K_2 . Figure 11 is a fit of the progress curve for active uptake at pH 7 (Fig. 3) by digital integration of the rate equation. We have assumed that Ca^{2+} is pumped in with the dependencies of Eq. (8), and that the net rate is diminished by a leak process with a first-order dependence on $[\text{Ca}^{2+}]_i$.

$$\text{Net rate} = V - k_{\text{leak}}[\text{Ca}^{2+}]_i \quad (13)$$

The fit was accomplished using the equilibrium and rate constants listed in Table 2. The rate constant for leakage (0.048 sec^{-1}) was adjusted to give an optimal fit of the data. Its value is larger than the value of 0.01 estimated for the $t_{1/2}$ of Ca^{2+} equilibration ($t_{1/2}=70$ to 700 sec) across the SR membrane in the absence of ATP in a previous study at 23°C (Chiu & Haynes, 1980*a*). The k_{leak} value is in line with the shorter $t_{1/2}$ values observed for passive Ca^{2+} equilibration in experiments under the present conditions at 30°C ($t_{1/2}$ approx. 20 sec; *data not shown*). The fit of theory to experiment is quite sensitive to the value of K_2 . High values of this parameter result in average rates and maximal steady-state uptakes which are too high, and vice versa. The fits of Figs. 9 and 10 are also sensitive to the choice of K_2 , but its value is not uniquely determined in those fits. The K_2 value of 5.4 mM gave an optimal fit for the data shown and for the progress curves at other $[\text{Ca}^{2+}]_o$ values (*not shown*). Figure 11 shows a systematic deviation between the calculated and experimental results, with the calculated values lagging behind experimental ones

in the initial phases of the reaction ($t=2$ sec). Excellent agreement in this time region is not expected since the model assumes that the enzyme is in the steady state, whereas this condition is probably not achieved until $t \geq 200$ msec. Also, the fit of the data could be improved with more accurate information on the inhibition of transport as a function of $[\text{Ca}^{2+}]_i$. We have assumed that an $E_i\text{Ca}_2$ complex is the only inhibitory species, but this may be an oversimplification.

The literature gives abundant evidence for Ca^{2+} occupation of the inwardly oriented translocator, but does not give a consensus on the question of whether the complex is 1:1 or 2:1. The data of Coan, Verjovski-Almeida and Inesi (1979) show that occupation of the low affinity site with 2Ca^{2+} induces a conformational change in the enzyme which can be read out by an ESR probe attached to SH groups. Ca^{2+} binding to the inwardly oriented translocator at millimolar concentrations has been demonstrated using a number of functional effects. These include the inhibition of ATP hydrolysis (Makinose & The, 1965; Weber et al., 1966; Ikemoto, 1974, 1975; de Meis & Carvalho, 1974; de Meis & Sorenson, 1975; Carvalho, Souza & de Meis, 1976), the decrease in ATP \leftrightarrow P_i exchange (de Meis & Carvalho, 1974; de Meis & Sorenson, 1975; Carvalho et al., 1976), the increase in steady-state phosphorylation with ITP (Souza & de Meis, 1976) and the decrease in the rate of phosphoenzyme dephosphorylation (Kanazawa et al., 1971; Yamada & Tonomura, 1972). With one exception, these studies do not speak to the question of whether a singly or doubly Ca^{2+} -occupied state is responsible for the effect. Inhibition of enzyme dephosphorylation, studied with the solubilized enzyme, has been shown to have a first-power dependence on the Ca^{2+} concentration (Yamada & Tonomura, 1972), suggesting that occupation of the inwardly oriented carrier by a single Ca^{2+} is allowed.

The question of the stoichiometry of the inhibitory complexes will be deferred to a future study. However, we believe that analysis using the present model gives a reasonable approximation to the progress curve for $[\text{Ca}^{2+}]_o \approx K_m$, pH 7.0. This analysis suggests that maximal steady-state uptake is achieved when $[\text{Ca}^{2+}]_i$ reaches a level such that the pump is severely inhibited and the rate of passive efflux equals the rate of pump-mediated influx.

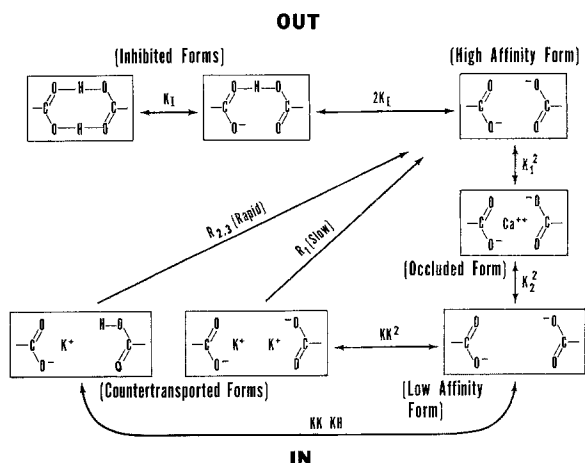
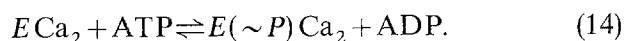


Fig. 12. Schematic representation of the Ca^{2+} translocator

Conformational Energetics of the Ca^{2+} Translocator

Consideration of the values of the constants derived from the present analysis allows us to make a number of deductions about the nature of the translocator site and the changes which it undergoes. The comparison of K_1 and K_2 is confirmatory of the findings of others that the pump undergoes a greater than three-order of magnitude decrease in affinity after translocation to the inside surface. The value of K_1 is chosen to equal the apparent binding constant found by Inesi et al. (1980) under passive conditions. The fitted K_2 value is in the range of the internal Ca^{2+} concentrations for half-maximal inhibition of ATPase function and phosphoenzyme decay reported in the studies cited in the previous section. In our simplified model, the processes of Eqs. (1) and (2) involve both enzyme phosphorylation and translocation which were implicitly assumed to have equilibrium constants of one. This assumption is reasonable to the extent that our K_1 and K_2 values are reasonable to the extent that our K_1 and K_2 values are reasonable. Experimental evidence for phosphorylation and translocation processes having equilibrium constants of approximately one has been given by Meissner (1973). He reported an equilibrium constant of 1.5 for the process:



His measurements were made at 0°C , pH 7.5 at Ca^{2+} concentrations sufficient to saturate both the outwardly and inwardly oriented translocators.

The K_m values observed for transport are substantially lower than K_d values reported for

passive binding (Inesi et al., 1980). The present model explains this difference by the effect of K^+ binding to the inwardly oriented translocator. We assume that K^+ does not bind to the outwardly oriented translocator. Thus under active transport conditions, increasing the K^+ concentration will increase the *apparent* affinity of the enzyme for Ca^{2+} by increasing the factor $F2\text{-}KK\text{-}KH$ (Eq. 10) and, by mass action, converting more enzyme into the inwardly oriented form. In absence of ATP, K^+ would be without effect on the apparent affinity.

Consideration of Translocator Architecture

A schematic model of translocator geometry is presented in Fig. 12. It incorporates features which explain the dramatic change in translocator affinity upon displacement from the outside to the inside, and it offers a reasonable explanation for the differences in H^+ affinity of the two forms deduced here. The model is in line with our tentative conclusions regarding the relative K^+ affinity of the two forms. According to the model, each translocator contains two COO^- groups in addition to a number of neutral liganding oxygens (*not pictured*). In the outwardly oriented form, the COO^- groups are in close proximity, optimal for inner sphere complexation of the Ca^{2+} (ionic radius = 0.99 \AA ; Weast & Selby, 1967). This separation is adequate for protonation, with high affinity due to the high negative charge density and the possibility of hydrogen bonding. The separation is not adequate for complexation of K^+ (ionic radius = 1.33 \AA). In the inwardly oriented form, the separation of the COO^- groups is larger and the translocator can complex all cations. The Ca^{2+} complexation occurs with three orders of magnitude lower affinity. The H^+ binding affinity is lowered due to the lower negative charge density and diminished opportunity for hydrogen bonding. Below, we will consider information on cation-ligand interaction which favors this model.

We believe that our findings on the pH dependence of K_{app} constitute strong evidence that the two translocators can be protonated with 2H^+ . Although this reaction could conceivably represent the protonation of neutral ligands, we consider it extremely unlikely that the Ca^{2+} translocator is neutral. We are not aware of any example of Ca^{2+} complexation with a stability constant of the order of $2.3 \times 10^6 \text{ M}^{-1}$ for neutral ligands in aqueous media. Consideration of Ca^{2+} binding in terms of cation-ligand interactions suggests that a -2

charge would make an important contribution to the binding affinity. The ligand EGTA, which has higher affinity than the translocator, bears a -2 charge at neutral pH (Chaborek & Martell, 1959; Martell & Smith, 1974). Its high affinity Ca^{2+} binding occurs with dissociation of 2H^+ to give a -4 charged form which combines with Ca^{2+} . Similarly, the high affinity of Ca^{2+} binding to arsenazo III depends on a high negative charge on the molecule (-5 or -6 ; cf. Chiu & Haynes, 1980c). Experience with Ca^{2+} ligands of high affinity and specificity suggests that both the negative charges and complexing groups must be optimally placed with respect to the complexed Ca^{2+} (Chaborek & Martell, 1959; Martell & Smith, 1974; Einspar & Bugg, 1977; Kretsinger, 1977). This would suggest that their complexing oxygens are closely packed at distances of the order of one atomic diameter of Ca^{2+} .

The inwardly oriented translocator has approximately three orders of magnitude lower Ca^{2+} affinity than the outwardly oriented translocator. This can be explained by the COO^- groups having acquired greater separation. K_a values on the order of 10^{-3} to 10^{-2} M are observed for Ca^{2+} complexes of a variety of carboxyl-containing compounds. The postulated configuration would allow for low-affinity Mg^{2+} complexation of the inwardly oriented translocator, as suggested by the findings that raising the Mg^{2+} concentration from 1 to 5 mM decreases the rate of transport (Froehlich & Taylor, 1975, 1976; Chiu & Haynes, 1980b).

Our analysis of the pH dependence of the K_{app} and V_m values gives values of 7.2 and 6.4 for the outwardly and inwardly oriented translocators, respectively. The $\text{p}K_a$ of 7.2 (outwardly oriented) could represent two closely packed and "buried" carboxyl groups, as depicted in Fig. 12. The affinity of the sites would be two orders of magnitude larger than for isolated carboxyl groups in an aqueous environment, due to the close packing, high negative charge density of the site, and opportunities for hydrogen bonding.

The present work arrives at a K^+ affinity constant (KK) of 30M^{-1} for each of the inwardly oriented negatively charged sites. This is a reasonable value for K^+ complexation of an isolated COO^- group in a semi-aqueous environment. The model assumes that only fully laden forms of the carrier are able to traverse the membrane, as expected for large energy barriers experienced in the movement of un-

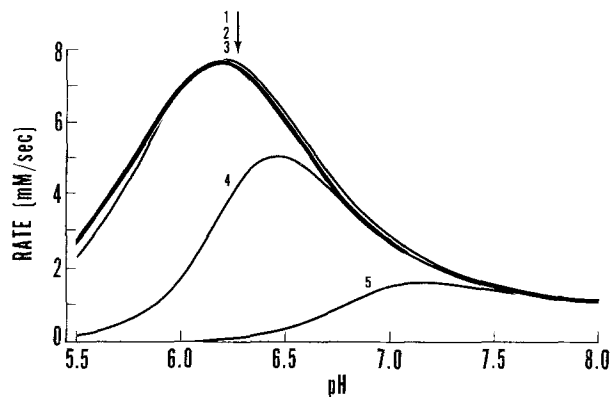


Fig. 13. pH dependence of the rate at various $[\text{Ca}^{2+}]_o$ levels. The computer program EQMOD was used for calculations. Constants were as given in Fig. 9 with $KH=1.5 \times 10^6\text{M}^{-1}$ and R_{1-5} values corresponding to the solid lines of Fig. 10. Curves 1-5 are calculations for the following $[\text{Ca}^{2+}]_o$ levels: 1.0×10^{-3} M, 1.0×10^{-4} M, 1.0×10^{-5} M, 1.0×10^{-6} M, and 1.0×10^{-7} M, respectively

compensated charge into a hydrophobic environment (Parsegian, 1969). To conform the model to the data, the rate constants for EHK_3 and EH_2K_2 translocation must be greater than that of EK_4 . This would seem to be reasonable since the COOH form has a higher degree of covalent character than the COOK complex. Also, the steric interactions between the COOH and COOK complexes might be more favorable than between two COOK complexes. Our data agrees with the findings of Chiesi and Inesi (1980) that one H^+ is exported per Ca^{2+} taken up at pH 6.0. The deduced relationship between the rate constants is also in line with the observation that $\text{E} \sim \text{P}$ hydrolysis occurs slowly at high pH.

pH Dependence of the Pump Under Physiological Conditions

The data of Fig. 7 show the ability of the pump to maintain a Ca^{2+} gradient for $[\text{Ca}^{2+}]_o = K_m$. Below pH 7.0, decreasing pH results in decreases in the gradient. This can be understood as the result of the greater pH dependence of K_{app} relative to that of V_m . Of greater interest to the physiological function of the pump would be its rate of pumping against an appreciable load ($[\text{Ca}^{2+}]_i = 3\text{mM}$) as a function of pH over a range of external Ca^{2+} concentrations. Figure 13 gives such a representation using the data of Table 2. The pH optimum of the pump shifts to more negative values as the external Ca^{2+} concentration is raised. Considered biophysically this is an expected consequence of the model and of the assumption of appreciable transinhibition. Considered phys-

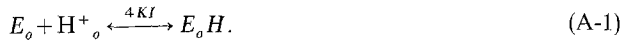
iologically, this form of pH dependence may represent an important mechanism for the minimization of damage in borderline ischemia. Damage occurs through a self-perpetuating cycle of contraction, metabolic compromise, elevated sarcoplasmic Ca^{2+} and metabolic acidosis. The data of Fig. 13 show that as the cytoplasmic Ca^{2+} is elevated, the pH optimum for Ca^{2+} accumulation shifts to lower values. This will introduce an element of negative feedback into the cycle enhancing the possibility of rescue.

We thank the journal referees for valuable comments and criticism and Miss Lori Link for invaluable assistance. This work was supported by NIH Grant GM23990 and by a grant from the Florida Heart Association.

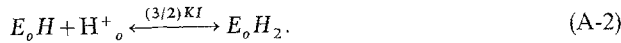
Appendix

Dependence of Average Rate on $[\text{H}^+]$, $[\text{K}^+]$, $[\text{Ca}^{2+}]_o$, $[\text{Ca}^{2+}]_i$

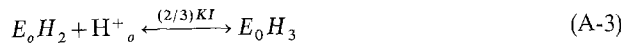
We assume that the two outwardly oriented translocators bind to Ca^{2+} in a cooperative manner (Inesi et al., 1980) according to Eq. (1) and that the enzyme is phosphorylated (Fig. 8). We further assume that the outwardly oriented carrier can bind H^+ to form an inhibitory complex. We define the intrinsic binding constant as KI , and assume that the binding constant for each of the four sites is independent of the degree of binding. The equilibrium constant for each sequential step must be weighted by a statistical factor accounting for the number of sites occupied in the reactant and product states. Thus the primary step proceeds as:



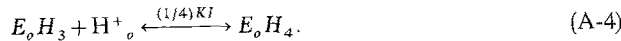
The equilibrium constant for this reaction is $4KI$, since the reactant translocator species have four sites available for H^+ binding and the product has one occupied site which can dissociate H^+ . Similarly, the next step in H^+ loading is:



The statistical factor $3/2$ is the result of the reactant species having three available sites and the product having two dissociable H^+ . Similarly, the third and fourth binding steps are:



and



We assume that only the fully Ca^{2+} -laden form of the translocator contributes to Ca^{2+} transport. This must be recognized as an approximation since we observed that lowering the pH to 5.5 results in a first-power dependence on $[\text{Ca}^{2+}]_o$. However, relaxation of this restriction to allow transport of $E_oH_2\text{Ca}$ complex would require a number of ancillary assumptions about relative binding constants and statistical factors which are not justified at this stage of the analysis.

The Ca^{2+} -laden form of the translocator dissociates Ca^{2+} in the SR lumen (Eq. 2). Next, the inwardly oriented

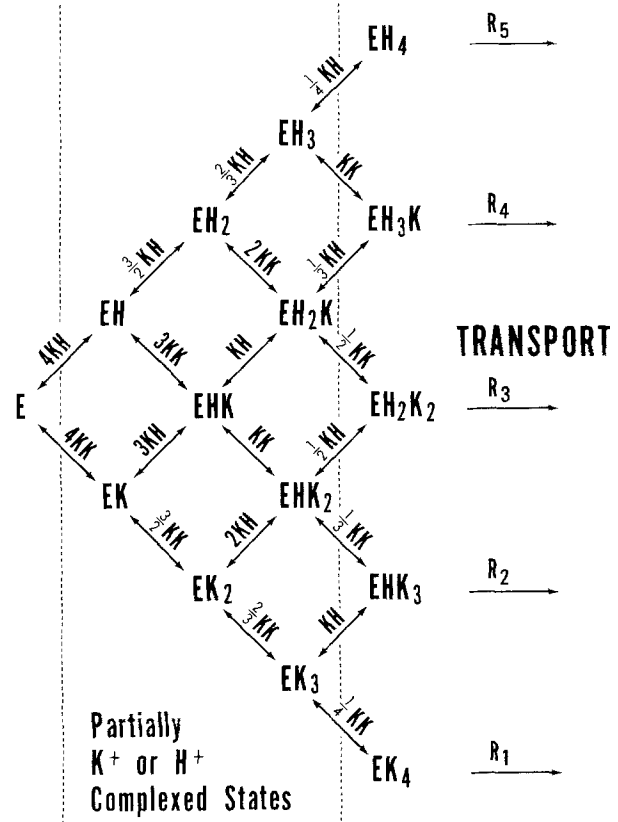


Fig. A1. Loading of the inwardly oriented translocator with K^+ and H^+

forms of the translocators are loaded with K^+ and H^+ . The protonation and K^+ binding equilibria of the inwardly oriented carrier are similar to those described in Eqs. (A-1)-(A-4) but are more complicated. The relationship between the process and the intrinsic binding constants for H^+ and K^+ (KH and KK , respectively) is given in Fig. (A-1). We assume that only the fully laden states are capable of translocation, and that the processes with rate constants R_{1-5} are rate-limiting. All other reactions are assumed to be in equilibrium. This assumption is probably not correct under all conditions of this study, but it affords great simplification of the kinetic analysis. Under the equilibrium assumption, the concentrations of all enzymatic species can be calculated from the equilibrium constants and reactant and product concentrations, using the principle of conservation of total enzyme. The latter is expressed as:

$$E_t = E_o + \sum_{n=1}^4 E_oH_n + E\text{Ca}_2 + \sum_{n=0}^4 \sum_{m=0}^{4-n} E_iK_mH_n \quad (\text{A-5})$$

where the concentration brackets are suppressed. This Equation is transformed into equations expressing the concentrations of the fully K^+ + H^+ laden inwardly oriented states, relative to the total enzyme. This is facilitated by defining constants which help to put Eq. (A-5) into overseable form. We define $F \cdot KI$ as:

$$F \cdot KI = \frac{E_o + \sum_{n=1}^4 E_oH_n}{E_o} \quad (\text{A-6})$$

Its value is given as:

$$(F-KI) = 1 + 4KI[H]_o + 6(KI[H]_o)^2 + 4(KI[H]_o)^3 + (KI[H]_o)^4 \quad (A-7)$$

The fourth and fifth terms in Eq. (A-5) are related using the constant $F2-KK-KH$ defined as:

$$F2-KK-KH = \frac{\sum_{n=0}^4 \sum_{m=0}^{4-n} E_i K_m H_n}{[E]_i} \quad (A-8)$$

Its value is given by:

$$(F2-KK-KH) = (1 + 4K(1 + (3/2)K(1 + (2/3)K(1 + K/4)))) + 4H(1 + 3K(1 + (2/2)K(1 + K/3))) + 4H^*(3/2)H((1 + 2K(1 + K/2)) + (2/3)H(1 + (H/4) + K)) \quad (A-9)$$

where K stands for $KK[K^+]_i$ and H represents $KH[H^-]_i$. This represents the totality of the partially and fully K^+ - and H^+ -laden forms of the inwardly oriented translocator. Equation (A-9) is structured in the same order as the double summation in Eq. (A-8). For ease of following the derivation, the constants have not been multiplied out and simplified. Equations (A-5), (A-7), (A-9), (1) and (2) were combined to give $[E_i K_n H_{5-n}]/[E]_i$ values. Noting that:

$$\text{Rate} = \frac{R_n [E_i K_n H_{5-n}]}{[E]_i} \quad (A-10)$$

we obtained:

$$\text{Rate} = \frac{(F1-KK-KH)(K_1[Ca]_o)^2}{((F2-KK-KH) + ([Ca]_i^2/K_2^2))(K_1[Ca]_o)^2 + 1} \cdot \frac{(F-KI)([Ca]_i^2/K_2^2)}{(F-KI)([Ca]_i^2/K_2^2)} \quad (A-11)$$

The Equation is seen to have a second-power Michaelis-Menten form with regard to $[Ca^{2+}]_o$. The value of $(F1-KK-KH)$ is given by:

$$(F1-KK-KH) = R_1(KK[K]_i)^4 + 4R_2(KK[K]_i)^3 + 6R_3(KK[K]_i)^2(KH[H]_i)^2 + 4R_4(KK[K]_i)(KH[H]_i)^3 + R_5(KH[H]_i)^4 \quad (A-12)$$

It gives the contribution of each of the K^+ + H^+ -laden forms of the inwardly oriented carrier to the rate. The R values are rate constants for translocation of each of the forms, expressed in terms of molar equivalents of Ca^{2+} in the lumen. The constant $(F2-KK-KH)$ expresses the effect of internal K^+ and H^+ totality of the Ca^{2+} -free inwardly oriented forms on the fraction of the enzyme in the countertransportable form.

The model makes predictions about the behavior of K_{app} and V_m for the average rate. The value of V_m is obtained for large $[Ca^{2+}]_o$:

$$V_m = \frac{(F1-KK-KH)}{(F2-KK-KH) + ([Ca]_i^2/K_2^2)} \quad (A-13)$$

This equation predicts that the V_m will depend on both $[K^+]_i$ and $[H^+]_i$. As the pH is decreased from 8.0 to 5.5 the V_m will shift sequentially from values characteristic of EK_4 to EHK_3 to EH_2K_2 to EH_3K to EH_4 . The value of K_{app} is given by:

$$K_{app} = K_1 \left(\frac{(F2-KK-KH) + ([Ca]_i^2/K_2^2)}{(F-KI)([Ca]_i^2/K_2^2)} \right)^{1/2} \quad (A-14)$$

At low pH values, the factor $F-KI$ would give a slope of 2 in Fig. 5. However, this can be partially offset by the $[H^+]_o$ dependence of $(F2-KK-KH)$ which increases with increasing protonation of the inwardly oriented carrier. The Discussion section shows that the pH dependence of K_{app} can be fit reasonably well with Eq. (A-14) under the assumption $KI \gg KH$. Equation (A-14) predicts that the value of K_{app} will be influenced by $[Ca^{2+}]_i$.

Prediction of the Time Course of Active Uptake

Equation (A-5) predicts that the rate of transport will be decreased with increasing $[Ca^{2+}]_i$. For both extremely high and low values of $[Ca^{2+}]_o$ the rate will be proportional to $1/[Ca^{2+}]_i^2$. At intermediate values of $[Ca^{2+}]_o$, a lower than -2 power dependence of the rate on $[Ca^{2+}]_i$ will be observed. The time course can be predicted from the model by integrating Eq. (A-11) with respect to $[Ca^{2+}]_i$, using small steps (1×10^{-5} M). In our modeling of the active uptake, we used:

$$d[Ca^{2+}]_i/dt = V - k_{leak}[Ca^{2+}]_i \quad (A-15)$$

where a nonspecific leakage process with a unimolecular rate constant k_{leak} is assumed. This assumption was made to accommodate our finding that Ca^{2+} will equilibrate slowly across the SR membrane under passive conditions (Chiu & Haynes, 1980a). Incorporation of this assumption results in finite values of $[Ca^{2+}]_i$ at infinite time. In practice, $[Ca^{2+}]_i$ was found to change only slowly for $t > 20$ sec, and the integration was truncated there.

References

- Berman, M.C., McIntosh, D.B., Kench, J.E. 1977. Proton inactivation of Ca^{2+} transport by sarcoplasmic reticulum. *J. Biol. Chem.* **252**:994-1000
- Carvalho, M.G.C., Leo, B.J. 1967. Effects of ATP on the interaction of Ca^{2+} , Mg^{2+} and K^+ with fragmented sarcoplasmic reticulum isolated from rabbit skeletal muscle. *J. Gen. Physiol.* **50**:1327-1352
- Carvalho, M.G.C., Souza, D.G., Meis, L. de 1976. On a possible mechanism of energy conservation in sarcoplasmic reticulum. *J. Biol. Chem.* **251**:3629
- Chaborek, S., Martell, A.E. 1959. Organic Sequestering Agents. John Wiley and Sons, New York
- Chiesi, M., Inesi, G. 1980. Adenosine 5'-triphosphate dependent fluxes of manganese and hydrogen ions in sarcoplasmic reticulum vesicles. *Biochemistry* **19**:2912-2918
- Chiu, V.C.K., Haynes, D.H. 1977. High and low affinity Ca^{2+} binding to the sarcoplasmic reticulum. *Biophys. J.* **18**:3-22
- Chiu, V.C.K., Haynes, D.H. 1980a. Rapid kinetic study of the passive permeability of a Ca^{2+} -ATPase rich fraction of the sarcoplasmic reticulum. *J. Membrane Biol.* **56**:203-218
- Chiu, V.C.K., Haynes, D.H. 1980b. Rapid kinetic studies of active Ca^{2+} transport in sarcoplasmic reticulum. *J. Membrane Biol.* **56**:219-239
- Chiu, V.C.K., Haynes, D.H. 1980c. The pH dependence and the binding equilibria of the calcium indicator Arsenazo III. *Membr. Biochem.* **3**:169-183
- Chiu, V.C.K., Mouring, D., Watson, B.D., Haynes, D.H. 1980. Measurement of surface potential and surface

- charge densities of sarcoplasmic reticulum membranes. *J. Membrane Biol.* **56**:121-132
- Coan, C., Verjovski-Almeida, S., Inesi, G. 1979. Ca²⁺ regulation of conformation of states in the transport cycle of spin-labelled sarcoplasmic reticulum ATPase. *J. Biol. Chem.* **254**:2968-2974
- Dixon, D., Corbett, A., Haynes, D.H. 1982. Effect of ATP/ADP phosphate potential on the maximal steady-state uptake of Ca²⁺ by skeletal sarcoplasmic reticulum. *J. Bioenerg. Biomembr.* **14**:87-96
- Einspar, H., Bugg, C.E. 1977. Crystal structures of calcium complexes of amino acids and related model systems. In: Calcium-Binding Proteins and Calcium Function. pp. 13-20. Elsevier-North Holland, New York
- Fabiato, A., Fabiato, F. 1978. Effects of pH on the myofilaments and the sarcoplasmic reticulum of skinned cells from cardiac and skeletal muscle. *J. Physiol. (London)* **276**:233-255
- Froehlich, J.P., Taylor, E.W. 1975. Transient state kinetic studies of sarcoplasmic reticulum adenosine triphosphatase. *J. Biol. Chem.* **250**:2013-2021
- Froehlich, J.P., Taylor, E.W. 1976. Transient state kinetic effects of calcium ion on sarcoplasmic reticulum adenosine triphosphatase. *J. Biol. Chem.* **251**:2307-2315
- Hasselbach, W. 1978. The reversibility of the sarcoplasmic reticulum calcium pump. *Biochim. Biophys. Acta* **463**:23-53
- Hasselbach, W., Makinose, M. 1963. Über den Mechanismus des Calciumtransportes durch die Membranen des sarkoplasmatischen Reticulums. *Biochem. Z.* **339**:94-111
- Haynes, D.H. 1982. Relationship between H⁺, anion, and monovalent cation movements and Ca²⁺ transport in sarcoplasmic reticulum. Further proof of a cation exchange mechanism for the Ca²⁺-Mg²⁺-ATPase pump. *Arch. Biochem. Biophys.* **215**:444-461
- Ikemoto, N. 1974. The calcium binding sites involved in the regulation of purified adenosine triphosphatase of the sarcoplasmic reticulum. *J. Biol. Chem.* **249**:649-651
- Ikemoto, N. 1975. Transport and inhibitory Ca²⁺ binding sites on the ATPase enzyme isolated from the SR. *J. Biol. Chem.* **250**:7219
- Inesi, G. 1972. Active transport of calcium ion in sarcoplasmic reticulum. *Annu. Rev. Biophys. Bioeng.* **1**:191-210
- Inesi, G., Croan, C., Verjovski-Almeida, S., Kurzmack, M., Lewis, D.E. 1978a. Mechanism of free energy utilization for active transport of calcium ion. In: Frontiers of Biological Energetics. L. Dutton, J. Lee and A. Scarpa, editors. Vol. II, pp. 1212-1219. Academic Press, New York
- Inesi, G., Kurzmack, M., Coan, C., Lewis, D.E. 1980. Cooperative calcium binding and ATPase activation in sarcoplasmic reticulum. *J. Biol. Chem.* **255**:3025-3031
- Inesi, G., Kurzmack, M., Verjovski-Almeida, S. 1978b. ATPase phosphorylation and calcium ion translocation in the transient state of sarcoplasmic reticulum activity. *Ann. N.Y. Acad. Sci.* **307**:224
- Kanazawa, T., Yamada, S., Yamamoto, T., Tonomura, Y.J. 1971. Reaction mechanism of Ca²⁺-dependent ATPase of sarcoplasmic reticulum from skeletal muscle. *J. Biochem.* **70**:95-123
- Kretsinger, R.H. 1977. Evolution of the informational role of calcium in eukaryotes. Calcium-Binding Proteins and Calcium Function. pp. 63-72. Elsevier-North Holland, New York
- MacLennan, D.H., Holland, P.C. 1975. Calcium transport in sarcoplasmic reticulum. *Annu. Rev. Biophys. Bioeng.* **4**:377-404
- Makinose, M., The, R. 1965. Calcium-Akkumulation und Nucleosidtriphosphat-Spaltung durch die Vesikel des sarcoplasmatischen Reticulum. *Biochem. Z.* **343**:383
- Martell, A.E., Smith, R.M. 1974. Critical Stability Constants, Vol. F: Amino Acids. Plenum Press, New York
- Masuda, H., Meis, L. de. 1973. Phosphorylation of the sarcoplasmic reticulum membrane by orthophosphate. Inhibition by calcium ions. *Biochemistry* **12**:4581-4585
- McKinley, D., Meissner, G. 1977. Sodium and potassium ion permeability of sarcoplasmic reticulum vesicles. *FEBS Lett.* **82**:47
- McKinley, D., Meissner, G. 1978. Evidence for a K⁺, Na⁺ permeable channel in sarcoplasmic reticulum. *J. Membrane Biol.* **44**:159-186
- Meis, L. de, Carvalho, M.G.C. 1974. Catalysis by sarcoplasmic reticulum. *Biochemistry* **13**:5032
- Meis, L. de, Sorenson, M.M. 1975. ATP Pi exchange and membrane phosphorylation in sarcoplasmic reticulum vesicles: Activation by silver in the absence of Ca²⁺ concentration gradient. *Biochemistry* **14**:2739
- Meis, L. de, Vianna, A.L. 1979. Energy interconversion by the Ca²⁺-dependent ATPase of the sarcoplasmic reticulum. *Annu. Rev. Biochem.* **48**:275-292
- Meissner, G. 1973. ATP and Ca²⁺ binding to the Ca²⁺ pump protein of sarcoplasmic reticulum. *Biochim. Biophys. Acta* **298**:906-929
- Meissner, G. 1975. Isolation and characterization of two types of sarcoplasmic reticulum vesicles. *Biochim. Biophys. Acta* **398**:51-68
- Parsegian, A. 1969. Energy of an ion crossing a low dielectric membrane: Solutions to four relevant electrostatic problems. *Nature (London)* **221**:344
- Riviero, J.M.C., Vianna, A.L. 1978. Allosteric modification by K⁺ of the (Ca²⁺+Mg²⁺)-dependent ATPase of sarcoplasmic reticulum: Interaction with Mg²⁺. *J. Biol. Chem.* **253**:3153-3157
- Shigekawa, M., Dougherty, J.P. 1978. Reaction mechanism of Ca²⁺-dependent ATP hydrolysis by skeletal muscle sarcoplasmic reticulum in the absence of added alkali metal salts. II. Kinetic properties of the phosphoenzyme formed at the steady-state in high Mg²⁺ and low Ca²⁺ concentrations. *J. Biol. Chem.* **253**:1451-1457
- Souza, D.G., Meis, L. de. 1976. Calcium and magnesium regulation of phosphorylation by ATP and ITP in sarcoplasmic reticulum. *J. Biol. Chem.* **251**:6355
- Tada, M., Yamamoto, T., Tonomura, Y. 1978. Molecular mechanism of active transport by sarcoplasmic reticulum. *Physiol. Rev.* **58**:1-79
- Verjovski-Almeida, S., Meis, L. de. 1977. pH-induced changes in the reactions controlled by the low- and high-affinity Ca²⁺ binding sites in sarcoplasmic reticulum. *Biochemistry* **16**:329-334
- Weast, R.C., Selby, S.M. 1967. Handbook of Chemistry and Physics. p.F-143. Chemical Rubber Company, Cleveland, Ohio
- Weber, A., Herz, R., Reiss, I. 1966. Study of the kinetics of calcium transport by isolated fragmented sarcoplasmic reticulum. *Biochem. Z.* **345**:329-369
- Yamada, S., Tonomura, Y. 1972. Reaction mechanism of the Ca²⁺-dependent ATPase of sarcoplasmic reticulum from skeletal muscle: VII. Recognition and release of Ca²⁺ ions. *J. Biol. Chem. (Tokyo)* **72**:417-425

Received 2 August 1982;

revised 26 October, 14 December 1982